



ISTITUTO NAZIONALE DI RICERCA METROLOGICA Repository Istituzionale

Comparative Study of Quasi-Solid-State Dye-Sensitized Solar Cells Using Z907, N719, Photoactive Phenothiazine Dyes and PVDF-HFP Gel Polymer Electrolytes with Different

Original

Comparative Study of Quasi-Solid-State Dye-Sensitized Solar Cells Using Z907, N719, Photoactive Phenothiazine Dyes and PVDF-HFP Gel Polymer Electrolytes with Different Molecular Weights / Afre, Rakesh A.; Ryu, Ka Yeon; Shin, Won Suk; Pugliese, Diego. - In: PHOTONICS. - ISSN 2304-6732. - 11:8(2024). [10.3390/photronics11080760]

Availability:

This version is available at: 11696/81559 since: 2024-09-05T06:19:16Z

Publisher:

MDPI

Published

DOI:10.3390/photronics11080760

Terms of use:

This article is made available under terms and conditions as specified in the corresponding bibliographic description in the repository

Publisher copyright

(Article begins on next page)

Article

Comparative Study of Quasi-Solid-State Dye-Sensitized Solar Cells Using Z907, N719, Photoactive Phenothiazine Dyes and PVDF-HFP Gel Polymer Electrolytes with Different Molecular Weights

Rakesh A. Afre ¹, Ka Yeon Ryu ², Won Suk Shin ³ and Diego Pugliese ^{4,*}

¹ Centre of Excellence in Nanotechnology (CoEN), Faculty of Engineering, Assam down town University (AdtU), Sankar Madhab Path, Gandhinagar, Panikhaiti, Guwahati, Assam 781026, India; rakesh.afre@adtu.in

² Research Institute of Molecular Alchemy, Gyeongsang National University, 501 Jinju-daero, Gyeongsangnam-do, Jinju-Si 52828, Republic of Korea; ryuky@gnu.ac.kr

³ Advanced Energy Materials Research Center, Korea Research Institute of Chemical Technology (KRICT), 141 Gajeong-ro, Yuseong-gu, Daejeon 34114, Republic of Korea; shinws@kRICT.re.kr

⁴ National Institute of Metrological Research (INRiM), Strada delle Cacce 91, 10135 Torino, Italy

* Correspondence: d.pugliese@inrim.it; Tel.: +39-011-3919-627

Abstract: The present study investigates the influence of photosensitizer selection and the polymer electrolyte composition on the performance of quasi-solid-state dye-sensitized solar cells (QsDSSCs). Two benchmark ruthenium dyes, N719 and Z907, alongside a novel photoactive phenothiazine dye were used. Each dye was incorporated into a QsDSSC architecture employing poly(vinylidene fluoride-co-hexafluoropropylene) (PVDF-HFP) as the gel electrolyte matrix, with varying molecular weights, to investigate their impacts on the overall device performance and long-term stability. Our results demonstrated that the N719 dye exhibited the highest power conversion efficiency (PCE), attributed to its strong absorption in the visible spectrum and efficient electron injection into the TiO₂ photoanode. Z907, on the other hand, showed moderate PCE due to its broader absorption profile but slower electron injection kinetics. The phenothiazine dye revealed promising PCE, with tunable absorption properties and efficient charge transfer. Furthermore, the impact of PVDF-HFP polymer gel electrolytes with varying molecular weights on cell stability was explored. The QsDSSC incorporating the PVH80 polymer with the phenothiazine dye exhibited reduced dye desorption, due to the effective dye molecules' immobilization by the gel matrix, and consequently enhanced long-term stability over 600 h. This comparative study sheds light on the interplay between dye selection, the polymer gel's properties, and QsDSSCs' performance. These insights are crucial in designing robust and efficient QsDSSCs for practical applications.

Keywords: dye-sensitized solar cells; ruthenium sensitizers; phenothiazine dyes; PVDF-HFP; stability study



Citation: Afre, R.A.; Ryu, K.Y.; Shin, W.S.; Pugliese, D. Comparative Study of Quasi-Solid-State Dye-Sensitized Solar Cells Using Z907, N719, Photoactive Phenothiazine Dyes and PVDF-HFP Gel Polymer Electrolytes with Different Molecular Weights. *Photonics* **2024**, *11*, 760. <https://doi.org/10.3390/photonics11080760>

Received: 21 June 2024

Revised: 31 July 2024

Accepted: 5 August 2024

Published: 14 August 2024



Copyright: © 2024 by the authors. Licensee MDPI, Basel, Switzerland. This article is an open access article distributed under the terms and conditions of the Creative Commons Attribution (CC BY) license (<https://creativecommons.org/licenses/by/4.0/>).

1. Introduction

The continuous escalation in the global energy demand, juxtaposed with the finite reserves of fossil fuels and the environmental necessity of curbing carbon emissions, has foregrounded the imperative need for renewable energy sources. Among these, solar energy stands as a prominent contender due to its ubiquity and sustainable nature. One promising photovoltaic technology that has witnessed significant advancement is the dye-sensitized solar cell (DSSC). Since its inception in 1991 by O'Regan and Grätzel, DSSCs have offered an attractive alternative to conventional p–n junction solar cells due to their lower manufacturing costs, ease of fabrication, potential for high energy conversion efficiency, and versatility in application [1–4].

Central to the DSSC architecture is the use of photosensitizers, which play a critical role by absorbing sunlight and facilitating electron injection from the excited dye molecule into the conduction band of a wide-bandgap semiconductor, typically titanium dioxide. Traditionally, ruthenium-based dyes such as N719 have been the industry standard, renowned for their broad absorption spectrum and efficient charge transfer properties. However, the scarcity of ruthenium and the quest for more sustainable options have stimulated research into alternative dyes, such as metal-free organic sensitizers like phenothiazine derivatives, which offer the benefits of lower costs and reduced environmental impacts [3,5,6]. A significant objective of this research is to overcome the reliance on rare and costly materials, such as ruthenium, while exploring the potential of novel organic photosensitizers that can offer competitive performance with enhanced sustainability and cost-effectiveness.

The classical archetype of a DSSC employs liquid electrolytes that include a redox mediator, usually iodide/tri-iodide (I_3^-/I^-), to shuttle electrons between the photoanode and the counter electrode. However, issues with liquid electrolyte volatilization, leakage, and degradation have led to the exploration of more robust alternatives, exemplified by quasi-solid-state electrolytes [7,8]. The latter present a balanced medium between liquid and solid states, aspiring to couple the inherent stability of the solid state with the superior ionic conductivity of the liquid state. Among the myriad of polymers used to form gel electrolytes, poly(vinylidene fluoride-co-hexafluoropropylene) (PVDF-HFP) has emerged as a preferential material due to its favorable attributes, which include a high dielectric constant, excellent photochemical stability, and suitability to host a variety of ionic liquids, which serve to enhance the ionic conductivity [5,9–11].

Our study aims to provide novel contributions in several key areas. In detail, our research provides a direct and systematic comparison of DSSCs' performance using two benchmark dyes (Z907 and N719) and a novel photoactive phenothiazine dye, combined with PVDF-HFP gel polymer electrolytes of varying molecular weights. This approach, unlike drawing conclusions from disparate reports, offers a clearer understanding of the interplay between the dye structure and electrolyte properties within a single study [12,13]. Additionally, particular emphasis was placed on long-term stability, systematically analyzing the performance evolution of each dye–electrolyte combination over an extended period. This focus on stability is crucial for real-world applications, providing valuable insights into long-term performance trends and degradation mechanisms. Finally, by examining the performance variations across different dye–electrolyte combinations, our study offers essential insights for material selection and optimization in DSSC fabrication, highlighting the importance of considering both individual components' properties and their synergistic interactions to achieve the desired performance and stability targets [14–17].

2. Materials and Methods

All reagents and solvents, unless otherwise specified, were obtained from Sigma-Aldrich (Seoul, Republic of Korea) and the Tokyo Chemical Industry Co., Ltd. (Tokyo, Japan), and used as received.

2.1. Substrate Preparation

Fluorine-doped tin oxide (FTO) glass substrates (MTI Korea, Seoul, Republic of Korea) with a thickness of 2 mm were first cleaned to remove surface contaminants. Cleaning involved sequential washing with soap water, deionized water, and then ethanol, followed by ultrasonication in ethanol for 20 min. The clean FTO substrates were then dried in a nitrogen flow. Post-cleaning, the FTO substrates were immersed in a 0.04 M titanium tetrachloride ($TiCl_4$) solution maintained at 70 °C for 30 min. This step was crucial to achieve a dense and uniform TiO_2 seed layer that facilitated the better adhesion of the mesoporous TiO_2 layer. After the pretreatment, the substrates were rinsed several times with deionized water to remove excess $TiCl_4$ and then dried.

2.2. TiO₂ Layer Deposition

For the deposition of the first TiO₂ base layer, a TiO₂ paste with a particle size <20 nm was prepared at KRICT, Daejeon, Republic of Korea, starting from in-house hydrothermally grown TiO₂ nanoparticles, and was spread over the FTO substrates using the screen-printing method. Then, 3M adhesive tape (3M Korea, Seoul, Republic of Korea) was employed to confine the coating area and an 11 µm screen was used to ensure uniformity in the layer thickness (10.5 µm). The printed substrates were dried by annealing at 125 °C for 30 min to remove organic components from the TiO₂ paste. Subsequently, a scattering layer (5.5 µm thick) composed of 400-nm-diameter TiO₂ particles (supplied by Dongjin Semichem Co., Ltd., Seoul, Republic of Korea) was added on top of the TiO₂ base layer utilizing a second screen-printing step. The substrates were then subjected to a sintering process with a temperature program as follows: pre-heating to 125 °C for 10 min, followed by incremental increases to 350 °C (5 min), 375 °C (5 min), and 450 °C (20 min). Finally, the temperature was ramped up to 500 °C and maintained for 10 min before allowing the substrates to cool down naturally to room temperature (RT). The final thickness of the TiO₂ films was assessed through a Dektak XT mechanical profilometer (Bruker, Tucson, AZ, USA) to be ~16 µm.

2.3. Photoelectrode and Counter Electrode Preparation

The prepared TiO₂ photoelectrodes underwent a post-synthesis conditioning step where they were immersed in a 0.1 M aqueous TiCl₄ solution. The temperature during this treatment was maintained at 70 °C for a duration of 30 min to enhance the surface properties of the TiO₂ films for better dye adsorption and electron transport. Following this treatment, the films were washed several times with deionized water to remove any residual TiCl₄ and were then dried. Subsequent to the TiCl₄ treatment, the TiO₂ films were sintered to ensure mechanical stability and to form effective electrical contact between the TiO₂ nanoparticles. The sintering was carried out in a programmable furnace with two distinct temperature holds: the films were first heated to 450 °C and maintained at this temperature for 20 min, followed by an increase to 500 °C for an additional 10 min. The sintered films were then allowed to cool down gradually to 80 °C. To prepare the counter electrode, H₂PtCl₆·6H₂O paste was deposited onto the FTO glass substrate using the screen-printing method and sintered in an electric muffle furnace at 300 °C for 15 min.

2.4. Photoelectrode Sensitization and Optical Characterization

The sintered TiO₂ electrodes were then immersed in 0.3 mM solutions of Z907, N719, and organic phenothiazine 2-LBH-92 dye in a tert-butyl alcohol and acetonitrile mixture at a 1:1 volume ratio. The electrodes were immersed overnight (>12 h) at room temperature and the conditions were optimized for each dye to ensure the maximum loading on the TiO₂ surface. The optical absorbance of the photoelectrodes sensitized with the three different dyes was obtained by an ultraviolet–visible (UV–Vis) spectrophotometer (UV-1800, Shimadzu Scientific Instruments, Kyoto, Japan).

2.5. Electrolyte Preparation

2.5.1. Liquid Electrolyte

The 1,2-dimethyl-3-propylimidazolium iodide (DMPII) liquid electrolyte (without polymer) was prepared by adding 0.1 M iodine (I₂), 0.5 M N-methylbenzimidazole (NMBI), and 0.6 M ionic liquid (IL)-DMPII in methoxypropionitrile (MPN) and by subsequent overnight stirring.

2.5.2. Gel Polymer Electrolytes

1. PVH70 (KRICT)—Molecular Weight (M.W.) 86,000 g/mol

First, 5 wt% PVH70 was added to MPN and stirred well at RT to obtain a clear polymer solution. Subsequently, 0.1 M I₂, 0.5 M NMBI, and 0.6 M IL-DMPII were added to the MPN and stirred overnight.

2. PVH80 (KRICT)—M.W. 90,000 g/mol

First, 5 wt% PVH80 was added to MPN and stirred well at RT to obtain a clear polymer solution. Subsequently, 0.1 M I₂, 0.5 M NMBI, and 0.6 M IL-DMPII were added to the MPN and stirred overnight.

3. PVDF-HFP (Sigma-Aldrich, Seoul, Republic of Korea)—M.W. 455,000 g/mol

First, 5 wt% PVDF-HFP was added to MPN and stirred well at 120 °C to obtain a clear polymer solution. Subsequently, 0.1 M I₂, 0.5 M NMBI, and 0.6 M IL-DMPII were added to the MPN and stirred overnight.

2.6. DSSC Assembly and Characterization

The DSSCs were assembled by sandwiching an electrolyte layer between the dye-sensitized TiO₂ photoelectrode and the counter electrode. A surlyn film (Solaronix, Aubonne, Switzerland) was used to maintain a gap between the two electrodes, thus ensuring the proper filling of the electrolyte. The electrolytes used were varied to examine their influence on the device performance: a DMPII liquid electrolyte and PVH70, PVH80, and PVDF-HFP gel polymer electrolytes.

The current density–voltage (*J*–*V*) curves of the devices were measured using a Keithley 2400 source measure unit (SMU) (Tektronix, Seoul, Republic of Korea) and a solar simulator (K201 LAB55, McScience Inc., Yeongtong, Republic of Korea). Irradiation of 100 mW/cm² with a 150 W xenon (Xe) short-arc lamp filtered by an air mass 1.5 G filter was used, which satisfied the Class AAA standard of the American Society for Testing and Materials (ASTM). The light intensity was calibrated with a Si reference cell (K801S-K302, McScience Inc.). The incident photon-to-electron conversion efficiency (IPCE) curves were measured using a spectral measurement system (K3100 IQX, McScience Inc.), which applied monochromatic light from a Xe arc lamp at 300 W, filtered by an optical chopper (MC2000, Thorlabs, Newton, NJ, USA) and a monochromator (CS130B-1-FH, Newport, Daejeon, Republic of Korea).

2.7. Stability Study of QsDSSCs

The stability study of the gel-polymer-electrolyte-based QsDSSCs with different molecular weights was performed by storing the cells at 70 °C in an oven with humidity of 40–45% and collecting data at 24 h intervals.

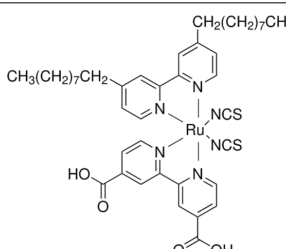
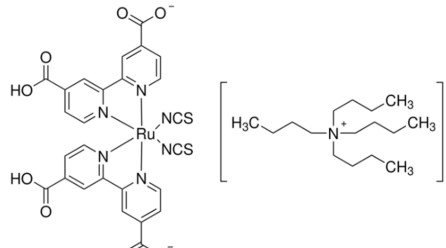
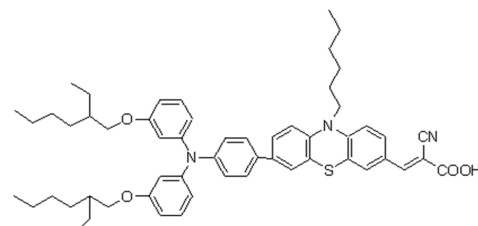
3. Results

3.1. Chemical Structures of the Dyes

Table 1 shows the chemical structures and names of the dyes used in this study: N719 and Z907 were purchased, while the organic phenothiazine dye was synthesized in our laboratory. N719 is known for its strong and broad absorption in the visible spectral range, which is crucial in capturing more sunlight. This dye displays a significant molar extinction coefficient, enabling efficient light harvesting with thinner films. N719 is chemically stable under DSSC operating conditions, ensuring the long-term performance of the solar cell. Moreover, it exhibits efficient charge transfer properties with rapid electron injection into the TiO₂ conduction band and quick dye regeneration by the redox mediator in the electrolyte. Z907 possesses enhanced thermal stability over N719, making it suitable for DSSCs operating at higher temperatures. Its molecular structure can be modified to fine-tune its photoelectronic properties for specific performance needs. The presence of longer aliphatic chains helps in forming a stable and hydrophobic layer on the semiconductor's surface, reducing charge recombination. Organic dyes like phenothiazine-based ones can have their electronic structures easily modified through chemical synthesis to obtain specific light absorption and charge transfer properties. Phenothiazine dyes are characterized by their extended π -conjugated systems, which enable strong absorption in the visible light range, essential for effective light harvesting in DSSCs. Similar to N719,

these organic dyes exhibit a high molar extinction coefficient, meaning that less material is required to absorb the same amount of light, helping to reduce the cell's cost [2].

Table 1. Chemical structures and names of Z907, N719, and organic phenothiazine dyes.

Chemical Structure	Chemical Name
	<p>cis-Bis(isothiocyanato)(2,2'-bipyridyl-4,4'-dicarboxylato)(4,4'-di-nonyl-2'-bipyridyl)ruthenium(II) (Z907 dye) M.W.: 870.10 g/mol</p>
	<p>Di-tetrabutylammonium cis-bis(isothiocyanato)bis(2,2'-bipyridyl-4,4'-dicarboxylato)ruthenium(II) (N719 dye) M.W.: 1188.55 g/mol</p>
	<p>(E)-3-(7-(4-(bis(3-((2-ethylhexyl)oxy)phenyl)amino)phenyl)-10-hexyl-10H-phenothiazin-3-yl)-2-cyanoacrylic acid (2-LBH-92) M.W.: 878.21 g/mol</p>

The designed molecule incorporates a donor–acceptor structure, which facilitates charge separation and transfer. The conjugated system between the donor and acceptor aids the electron flow from the excited dye to the semiconductor. The structures of organic dyes allow for significant modifications of their molecular structures to optimize their photophysical and electrochemical properties for better performance. The solubility of organic dyes in common organic solvents is beneficial for the preparation of dye solutions and can influence the quality of the dye-sensitized semiconductor's surface. Phenothiazine dyes often display reduced aggregation on semiconductor surfaces compared to other organic dyes, which can lead to improved electron injection efficiency and reduced charge recombination. Properly designed phenothiazine dyes can also exhibit good stability, which is crucial for the long-term operation of DSSCs. These properties of the phenothiazine dye contribute to the overall performance of DSSCs when employed as the sensitizing agent. In the context of our comparative study, the interaction of this dye with PVDF-HFP gel polymer electrolytes with different molecular weights would allow for a thorough analysis of the dynamics within the quasi-solid-state environment of the DSSC and an assessment of the impact of these interactions on the device performance parameters, such as the efficiency, photostability, and charge transport mechanism.

3.2. J–V Characteristics of DSSCs with Z907, N719, and Phenothiazine Dye and with and without PVDF-HFP with Different Molecular Weights in DMPII Electrolyte

Table 2 summarizes the main photovoltaic parameters at day 1 (day of cell assembly), day 2 (after 24 h), and day 3 (after 48 h) for the DSSCs based on the Z907, N719, and organic phenothiazine dyes with DMPII liquid electrolytes in the presence and in the absence of

PVDF-HFP polymers with different molecular weights; the corresponding $J-V$ curves are reported in Figure 1.

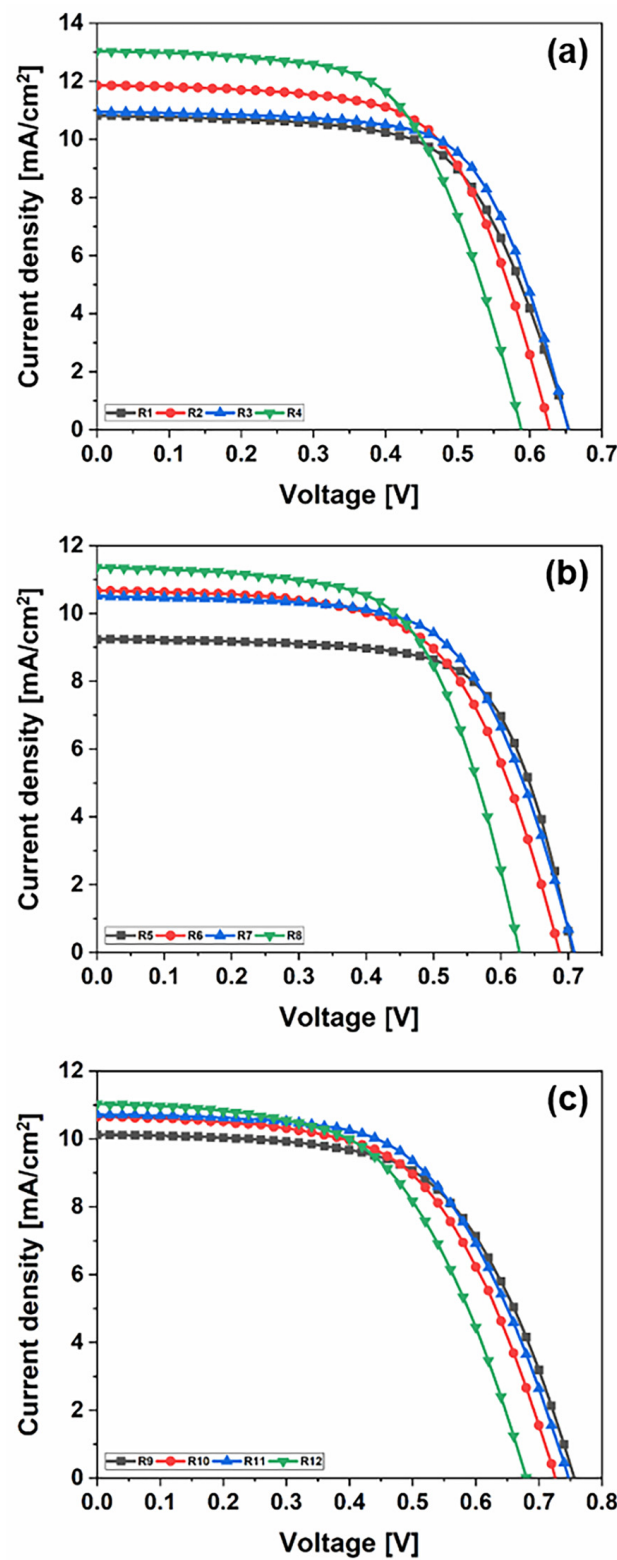


Figure 1. $J-V$ characteristics of DSSCs using liquid DMPII electrolytes with and without PVDF-HFP with different molecular weights and (a) Z907, (b) N719, and (c) organic phenothiazine 2-LBH-92 dyes as the sensitizer.

Table 2. Main photovoltaic parameters of DSSCs using Z907, N719, and 2-LBH-92 as the sensitizer and DMPII with and without PVDF-HFP with a different molecular weight as the electrolyte.

Sample No.	Dye	Electrolyte	Day 1				Day 2				Day 3			
			V_{oc} [V]	J_{sc} [mA/cm ²]	FF	PCE [%]	V_{oc} [V]	J_{sc} [mA/cm ²]	FF	PCE [%]	V_{oc} [V]	J_{sc} [mA/cm ²]	FF	PCE [%]
R1	Z907	DMPII liq.	0.65	10.80	0.64	4.53	0.66	10.41	0.66	4.55	0.66	10.33	0.66	4.51
R2		PVH70	0.63	11.85	0.64	4.74	0.64	11.37	0.65	4.74	0.65	10.99	0.65	4.71
R3		PVH80	0.65	10.96	0.67	4.77	0.66	10.55	0.66	4.61	0.66	10.51	0.66	4.62
R4		PVDF-HFP	0.59	13.03	0.61	4.68	0.61	11.87	0.62	4.52	0.62	11.05	0.63	4.35
R5	N719	DMPII liq.	0.71	9.23	0.69	4.47	0.79	9.33	0.69	4.67	0.73	9.27	0.69	4.67
R6		PVH70	0.69	10.67	0.61	4.48	0.70	10.36	0.66	4.79	0.71	10.17	0.66	4.76
R7		PVH80	0.71	10.51	0.63	4.72	0.72	10.35	0.68	5.06	0.73	10.26	0.68	5.12
R8		PVDF-HFP	0.63	11.36	0.62	4.45	0.64	9.56	0.66	4.03	0.65	8.59	0.68	3.83
R9	2-LBH-92	DMPII liq.	0.76	10.12	0.60	4.59	0.77	9.82	0.62	4.71	0.78	9.81	0.62	4.74
R10		PVH70	0.73	10.65	0.59	4.48	0.75	10.56	0.58	4.36	0.76	10.21	0.58	4.54
R11		PVH80	0.75	10.72	0.58	4.69	0.76	10.75	0.61	5.07	0.77	10.72	0.61	5.01
R12		PVDF-HFP	0.68	11.03	0.56	4.20	0.68	10.12	0.57	3.92	0.67	8.98	0.57	3.42

Cells R1–R4: Z907 dye

On day 1, the DSSCs using the Z907 dye exhibited diverse performance metrics. Sample R1, employing a liquid electrolyte, showed a V_{oc} of 0.65 V, a J_{sc} of 10.80 mA/cm², an FF of 0.64, and efficiency (PCE) of 4.53%. Comparatively, sample R2 with the PVH70 electrolyte exhibited a slightly lower V_{oc} of 0.63 V but a higher J_{sc} of 11.85 mA/cm² and a similar FF of 0.64, resulting in higher PCE of 4.74%. Sample R3 with the PVH80 electrolyte presented a V_{oc} of 0.65 V, a J_{sc} of 10.96 mA/cm², an improved FF of 0.67, and PCE of 4.77%. Finally, sample R4 with the PVDF-HFP electrolyte achieved a lower V_{oc} of 0.59 V but the highest J_{sc} of 13.03 mA/cm², an FF of 0.61, and PCE of 4.68%. The average values with the relative uncertainty of the photovoltaic parameters of the Z907 DSSCs evaluated on day 1 are therefore equal to $V_{oc} = (0.63 \pm 0.03)$ V, $J_{sc} = (11.66 \pm 0.98)$ mA/cm², $FF = 0.64 \pm 0.03$, and $PCE = (4.68 \pm 0.10)\%$. Over three days, the performance metrics showed slight variations. By day 3, R1 showed PCE of 4.51%, R2 of 4.71%, R3 of 4.62%, and R4 showed a decrease to 4.35%. The primary observation is that the PVDF-HFP electrolyte, despite its high J_{sc} , suffers from a lower V_{oc} and FF, leading to less stable efficiency compared to the other electrolytes.

Cells R5–R8: N719 dye

The N719 dye-based DSSCs displayed a different performance profile. On day 1, sample R5 with a liquid electrolyte recorded a V_{oc} of 0.71 V, a J_{sc} of 9.23 mA/cm², an FF of 0.69, and PCE of 4.47%. Sample R6 using the PVH70 electrolyte improved the J_{sc} to 10.67 mA/cm² but had a lower FF of 0.61, yielding PCE of 4.48%. Sample R7 with PVH80 showed a similar V_{oc} of 0.71 V, a J_{sc} of 10.51 mA/cm², an improved FF of 0.63, and higher PCE of 4.72%. Sample R8 using the PVDF-HFP electrolyte displayed a V_{oc} of 0.63 V, a J_{sc} of 11.36 mA/cm², an FF of 0.62, and PCE of 4.45%. The average values with the relative uncertainty of the photovoltaic parameters of the N719 DSSCs evaluated on day 1 are therefore equal to $V_{oc} = (0.69 \pm 0.03)$ V, $J_{sc} = (10.44 \pm 0.88)$ mA/cm², $FF = 0.64 \pm 0.03$, and $PCE = (4.53 \pm 0.12)\%$. Over three days, R5's efficiency increased to 4.67%, indicating good stability. R6 and R7 showed improved PCE of 4.76 and 5.12%, respectively, by day 3. However, R8 experienced a significant drop in PCE to 3.83% by day 3, suggesting that while PVDF-HFP provided a higher initial J_{sc} , it suffered from stability issues over time.

Cells R9–R12: Phenothiazine dye

The phenothiazine dye-based DSSCs highlighted promising initial results. On day 1, sample R9 with a liquid electrolyte showed a V_{oc} of 0.76 V, a J_{sc} of 10.12 mA/cm², an FF of 0.60, and PCE of 4.59%. Sample R10 with the PVH70 electrolyte exhibited a V_{oc} of 0.73 V, a J_{sc} of 10.65 mA/cm², an FF of 0.59, and PCE of 4.48%. Sample R11 using PVH80 achieved a V_{oc} of 0.75 V, a J_{sc} of 10.72 mA/cm², an FF of 0.58, and PCE of 4.69%. Finally, sample R12 with the PVDF-HFP electrolyte recorded a V_{oc} of 0.68 V, a J_{sc} of 11.03 mA/cm², an FF of 0.56, and PCE of 4.20%. The average values with the relative uncertainty of the photovoltaic parameters of the phenothiazine DSSCs evaluated on day 1 are therefore equal to

$V_{oc} = (0.73 \pm 0.04)$ V, $J_{sc} = (10.63 \pm 0.38)$ mA/cm², FF = 0.58 ± 0.02 , and PCE = (4.49 ± 0.18) %. By day 3, sample R9's efficiency slightly increased to 4.74%, indicating good stability. Samples R10 and R11 showed improved PCE of 4.54 and 5.01%, respectively, with R11 showing the best stability and efficiency among the phenothiazine dye group. However, sample R12's PCE dropped significantly to 3.42%, mirroring the trend observed with other PVDF-HFP electrolyte-based cells.

Across all three groups, the choice of electrolyte had a significant impact on the performance and stability of the DSSCs. The PVDF-HFP electrolyte, while providing a high initial J_{sc} , generally resulted in lower stability and efficiency over time compared to the PVH70 and PVH80 electrolytes. This comparative study highlights the critical role of electrolyte selection in optimizing the performance and durability of DSSCs.

The performance of QsDSSCs can be significantly impacted also by the choice of photosensitizer dye, such as Z907, N719, and organic phenothiazine 2-LBH-92; below, some aspects revealing how these dyes influence the DSSC performance are reported.

Each dye displays a characteristic absorption spectrum. For instance, N719 is a ruthenium-based complex known for its broad and strong absorption in the visible spectrum and good performance in both liquid and QsDSSCs. Z907 is also a ruthenium complex but with slightly different ligands, which might absorb light differently from N719, potentially impacting the cell's light-harvesting efficiency. Organic phenothiazine dyes, such as the one mentioned, absorb light based on their conjugated systems and can be tuned to enhance their light absorption over specific wavelength ranges. The molecular architectures of these dyes determine their ability to anchor to the TiO₂ surface, resist aggregation, and avoid steric hindrance, all of which can affect the electron injection efficiency and charge recombination rates.

The dyes' different energy levels might exhibit varying alignment with the conduction band of TiO₂. The energy level alignment determines the efficiency and the driving force for the transfer of electrons from the dye to the semiconductor upon photoexcitation. Ruthenium dyes such as N719 and Z907 generally show good energy level alignment, yielding efficient electron injection [18]. Organic phenothiazine dyes might have different energy level alignment, which can also result in efficient electron injection, but they might require careful design to optimize their performance within a QsDSSC.

Some dyes are more stable than others when exposed to light and the DSSC operating environment. Organic phenothiazine dyes may offer higher molar extinction coefficients but can be less stable than ruthenium-based dyes under prolonged exposure to lighting conditions. Efficient charge separation in DSSCs requires that the oxidized dye molecule is effectively reduced by the redox mediator in the quasi-solid-state electrolyte. The redox potential of the dye in its oxidized state should match well with the potential of the redox couple used in the electrolyte. Ruthenium dyes like N719 and Z907 are well matched with the conventional iodide/triiodide redox couple, facilitating effective dye regeneration without much energy loss. For organic phenothiazine dyes, their redox potentials might be different, and the match with the redox mediator needs to be good to ensure efficient regeneration and to prevent potential losses that could reduce the cell's voltage.

The interaction between the dye and the TiO₂ surface influences the electron lifetime and recombination dynamics. Dyes that adsorb strongly to TiO₂ and form an optimal monolayer can inhibit charge recombination and extend electron lifetimes. In the case of N719 and Z907, the strong anchoring groups and larger molecules might provide good coverage and passivation on the TiO₂ surface. The molecular design of phenothiazine dyes usually includes anchoring groups like the cyanoacrylic acid moiety, which can provide similar benefits, but might require optimization for the specific quasi-solid-state system.

Overall, the dye choice for QsDSSCs should consider factors like light absorption, the energy levels, the stability under operational conditions, and the interfacial electron dynamics to maximize the photovoltaic performance and longevity. Each dye brings a unique set of advantages and challenges in terms of efficiency, stability, and fabrication requirements.

3.3. DSSCs with Z907 Dye and with and without PVDF-HFP with Different Molecular Weights in DMPII Electrolyte

3.3.1. UV-Vis Absorption and IPCE Spectra

The UV-Vis absorption spectrum of the Z907 dye typically exhibits two characteristic bands: a strong absorption peak in the UV region at around 300 nm, attributed to π - π^* transitions within the bipyridine ligands, and a broader absorption band in the visible region, peaking around 530 nm, arising from metal-to-ligand charge transfer (MLCT) transitions (Figure 2a). Incorporating PVDF-HFP into the electrolyte, which comprises 0.1 M I_2 , 0.5 M NMBI, and 0.6 M IL-DMPII, can influence the dye's absorption behavior. For instance, interactions between the dye molecules and the polymer chains might lead to slight shifts in the absorption peaks or changes in peak intensity. These spectral variations can provide insights into the degree of dye aggregation, which can negatively impact device performance by increasing charge recombination.

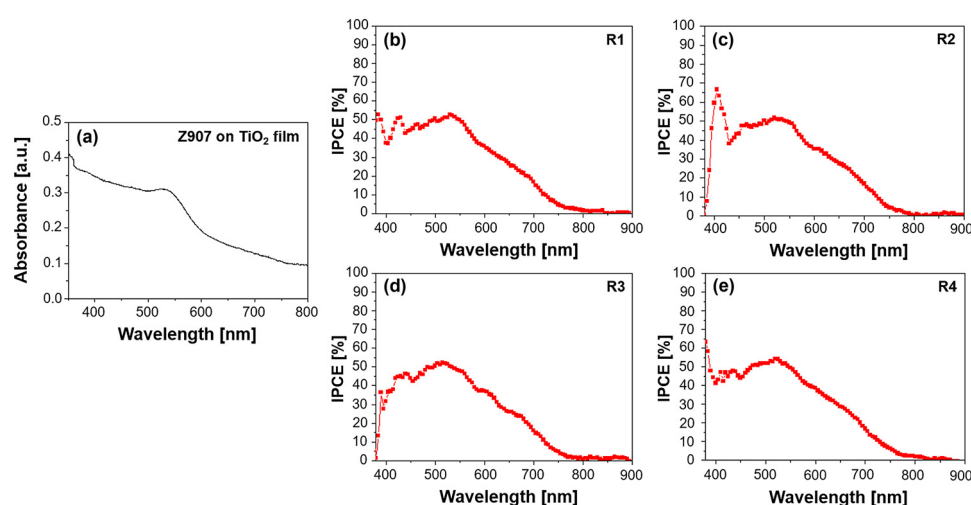


Figure 2. (a) UV-Vis absorption spectrum of Z907 dye on TiO₂ film and quantum efficiency spectra for (b) R1—DMPII, (c) R2—DMPII + PVH70, (d) R3—DMPII + PVH80, and (e) R4—DMPII + PVDH-HFP Z907 sensitized solar cells.

The IPCE spectra offer a more direct measure of the DSSC's ability to convert incident photons into an electrical current. Z907 typically exhibits a broad IPCE spectrum, mirroring its absorption profile, with the maximum efficiency often observed at around 530 nm. The presence of PVDF-HFP in the electrolyte can significantly influence the IPCE spectrum (see Figure 2b–e). Different molecular weights of the polymer can lead to variations in the electrolyte's viscosity and ionic conductivity, ultimately affecting the charge transport within the device. For instance, a high-molecular-weight PVDF-HFP might result in a more viscous electrolyte, hindering ion diffusion and potentially reducing the IPCE, particularly at longer wavelengths, where the charge collection efficiency becomes more critical. Conversely, a lower-molecular-weight PVDF-HFP might lead to a less viscous electrolyte, facilitating ion transport and potentially enhancing the IPCE. However, the optimal molecular weight represents a balance, as excessively low molecular weights might compromise the quasi-solid-state nature of the electrolyte, impacting the long-term stability [19].

Furthermore, the interaction between the Z907 dye and the PVDF-HFP polymer can influence the electron injection and dye regeneration processes. For example, if the polymer interacts favorably with the dye's excited state, it could facilitate electron injection into the TiO₂ conduction band, leading to an increased IPCE. Conversely, unfavorable interactions could hinder these processes, negatively impacting the device's performance. In conclusion, analyzing the UV-Vis absorption and IPCE spectra of Z907-sensitized QsDSSCs with varying molecular weights of PVDF-HFP in the electrolyte provides valuable information

about the dye–electrolyte interactions, charge transport properties, and overall device performance. Understanding these relationships is crucial in optimizing the electrolyte composition and device architecture to achieve high efficiency and long-term stability in DSSC applications.

Several factors could have contributed to the observation of the unusually high IPCE below 400 nm as shown in Figure 2e; they were actively investigated to try to provide a conclusive explanation. One possible factor is the scattering effects caused by the TiO₂ nanoparticles used in the photoanode. These nanoparticles can scatter light, especially in the UV region, leading to the overestimation of the IPCE in this wavelength range. Scattered photons might be detected multiple times or contribute to the photocurrent through indirect pathways, thus inflating the IPCE values. Another potential factor is measurement artifacts. Despite taking precautions to ensure accurate IPCE measurements, instrumental artifacts or limitations in the calibration of the light source and detector in the UV region could have contributed to the observed high values. Our measurement setup and protocols were thoroughly verified to rule out any systematic errors. Additionally, although less likely, the possibility of dye aggregation on the TiO₂ surface cannot be entirely ruled out. If dye aggregates are present, they could exhibit altered optical properties, potentially leading to enhanced absorption and IPCE in the UV region.

3.3.2. Stability Study

The stability study of the Z907-sensitized solar cells with the liquid DMPII electrolyte and with gel polymer electrolytes with different molecular weights is shown in Figure 3. In this context, the stability study of QsDSSCs employing the Z907 dye and electrolytes with varying molecular weights of the PVDF-HFP polymer can reveal how these factors influence the durability and overall performance over time. In our research setup, cells R1, R2, R3, and R4 exhibited different trajectories after over 600 h of operation, indicating the complex influence of the PVDF-HFP polymer’s molecular weight within the context of a QsDSSC.

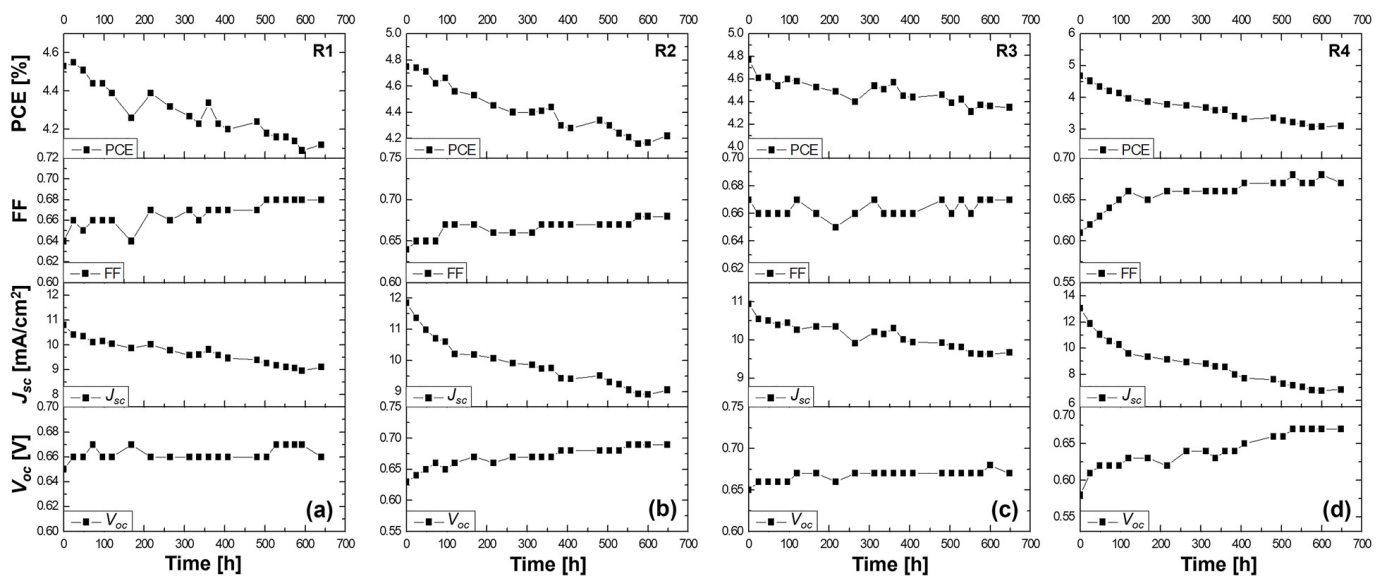


Figure 3. Stability study for more than 600 h at ambient conditions of the (a) R1 DSSC based on the DMPII liquid electrolyte and of the QsDSSCs using PVDF-HFP with different molecular weights: (b) R2—DMPII + PVH70, (c) R3—DMPII + PVH80, and (d) R4—DMPII + PVDH-HFP. All solar cells were sensitized with the Z907 dye.

R1 cell (liquid DMPII electrolyte)

The R1 cell, utilizing a liquid DMPII electrolyte, exhibited a 9% decrease in overall efficiency after 600 h. This decline primarily stemmed from a 15% reduction in the J_{sc} ,

suggesting potential issues with electron injection, dye regeneration, or charge transport within the device. However, the V_{oc} and FF showed slight improvements of 1.5 and 1%, respectively. This V_{oc} increase could indicate reduced recombination losses, possibly due to passivation effects at the $\text{TiO}_2/\text{dye}/\text{electrolyte}$ interface over time. The slight FF improvement might be attributed to changes in the electrolyte composition or interface properties that enhance charge collection.

R2 cell (PVDF-HFP electrolyte with M.W. of 86,000 g/mol)

Incorporating PVDF-HFP polymers into the electrolyte significantly influenced the devices' stability. The R2 cell, with a polymer molecular weight of 86,000 g/mol, displayed an 11% efficiency reduction after 600 h. While this decrease is comparable to that of the R1 cell, the individual parameter changes differed. The R2 cell exhibited a more pronounced V_{oc} increase of 10%, suggesting a more substantial reduction in recombination losses, potentially due to the polymer's ability to suppress interfacial charge recombination. However, the J_{sc} experienced a more significant decline of 24%, indicating that the polymer might hinder charge transport or negatively impact dye regeneration. The FF showed a notable improvement of 7%, likely due to the polymer's influence on the electrolyte's ionic conductivity and interfacial properties.

R3 cell (PVDF-HFP electrolyte with M.W. of 90,000 g/mol)

The R3 cell, employing a slightly higher molecular weight of PVDF-HFP (90,000 g/mol), demonstrated a 9% efficiency reduction after 600 h, similar to the R1 cell. This cell exhibited a moderate V_{oc} increase of 4%, a slight FF improvement of 1%, and a J_{sc} decrease of 13%. These results suggest that this specific polymer molecular weight might offer a balance between suppressing recombination and maintaining reasonable charge transport properties.

R4 cell (PVDF-HFP electrolyte with M.W. of 455,000 g/mol)

The R4 cell, incorporating the highest molecular weight of PVDF-HFP (455,000 g/mol), suffered the most significant efficiency loss, plummeting by 33% after 600 h. This dramatic decline primarily resulted from the substantial 50% drop in the J_{sc} , indicating severe limitations in charge transport within the device. The high-molecular-weight polymer likely formed a dense network within the electrolyte, hindering ion diffusion and significantly impeding charge collection. Despite the substantial V_{oc} increase of 14%, likely due to suppressed recombination, and a notable FF improvement of 9%, the severe J_{sc} limitation ultimately dominated the device's performance degradation.

This stability study highlights the complex interplay between the electrolyte composition, polymer molecular weight, and device performance in QsDSSCs. While liquid electrolytes might suffer from limitations related to long-term stability and potential leakage, incorporating PVDF-HFP polymers introduces a trade-off between enhancing the stability and maintaining efficient charge transport. Lower-molecular-weight polymers appear to offer a better balance, preserving reasonable charge transport while mitigating some of the drawbacks associated with liquid electrolytes. However, excessively high molecular weights can severely hinder ion diffusion, leading to significant performance losses despite potential improvements in other parameters. Optimizing the polymer molecular weight and electrolyte composition is crucial in achieving efficient QsDSSCs that are stable in the long term.

3.4. DSSCs with N719 Dye and with and without PVDF-HFP with Different Molecular Weights in DMPII Electrolyte

3.4.1. UV-Vis Absorption and IPCE Spectra

In the field of DSSCs, evaluating the UV-Vis absorption and IPCE spectra is crucial to optimize the device performance (see Figure 4). Analyzing these spectra for the N719 dye incorporated into both quasi-solid-state and liquid DSSCs, i.e., with and without PVDF-HFP polymers of varying molecular weights in the electrolyte (0.1 M I_2 , 0.5 M NMBI, and 0.6 M IL-DMPII), can elucidate the impact of the polymer on the dye's light-harvesting capabilities and charge generation processes [20].

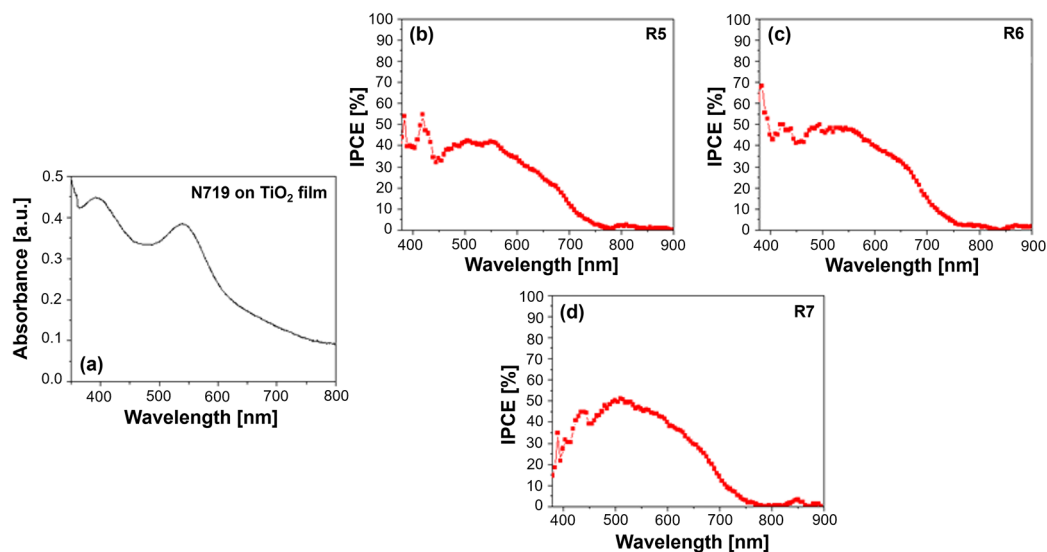


Figure 4. (a) UV–Vis absorption spectrum of N719 dye on TiO₂ film and quantum efficiency spectra for (b) R5—DMPII, (c) R6—DMPII + PVH70, and (d) R7—DMPII + PVH80 N719 sensitized solar cells. The quantum efficiency data of the R8—DMPII + PVDH-HFP cell are not available due to the degradation of the device.

N719, a ruthenium-based dye, typically exhibits two prominent absorption bands in its UV–Vis spectrum (see Figure 4a). A strong absorption peak at around 390 nm arises from MLCT transitions within the dye molecule. A broader absorption band, peaking at around 530 nm, also originates from MLCT transitions but involves a different energy level within the dye’s molecular orbital structure. Incorporating PVDF-HFP into the electrolyte can influence the dye’s absorption behavior. Interactions between the dye molecules and the polymer chains might induce slight shifts in the absorption peaks or alter the peak intensities. These spectral variations can provide insights into the degree of dye aggregation, which can negatively impact device performance by increasing charge recombination [2,9].

The IPCE spectra offer a more direct measure of the DSSC’s ability to convert incident photons into an electrical current. N719 typically exhibits a broad IPCE spectrum, mirroring its absorption profile, with the maximum efficiency observed around the wavelengths corresponding to its MLCT absorption bands. The presence of PVDF-HFP in the electrolyte can significantly influence the IPCE spectrum (see Figure 4b–d). Different molecular weights of the polymer can lead to variations in the electrolyte’s viscosity and ionic conductivity, ultimately affecting the charge transport within the device.

For instance, a high molecular weight of PVDF-HFP might result in a more viscous electrolyte, hindering ion diffusion and potentially reducing the IPCE, particularly at longer wavelengths, where the charge collection efficiency becomes more critical. Conversely, a lower molecular weight of PVDF-HFP might lead to a less viscous electrolyte, facilitating ion transport and potentially enhancing the IPCE. However, the optimal molecular weight represents a balance, as excessively low molecular weights might compromise the quasi-solid-state nature of the electrolyte, impacting the long-term stability [21–23].

Furthermore, the interaction between the N719 dye and the PVDF-HFP polymer can influence the electron injection and dye regeneration processes. For example, if the polymer interacts favorably with the dye’s excited state, it could facilitate electron injection into the TiO₂ conduction band, leading to increased IPCE. Conversely, unfavorable interactions could hinder these processes, negatively impacting the device’s performance.

3.4.2. Stability Study

This stability study focuses on understanding the long-term performance of DSSCs utilizing the N719 dye and various electrolytes. The changes in the V_{oc} , FF, J_{sc} , and overall efficiency after a 600 h aging period will be thoroughly analyzed. Our analysis en-

compasses a control cell (R5) with a liquid DMPII electrolyte and cells incorporating PVDF-HFP polymers of different molecular weights (R6: 86,000 g/mol, R7: 90,000 g/mol, R8: 455,000 g/mol) in the electrolyte.

The long-term stability data for the N719-sensitized solar cells with the liquid DMPII electrolyte and various molecular weights of the PVDF-HFP polymer are shown in Figure 5.

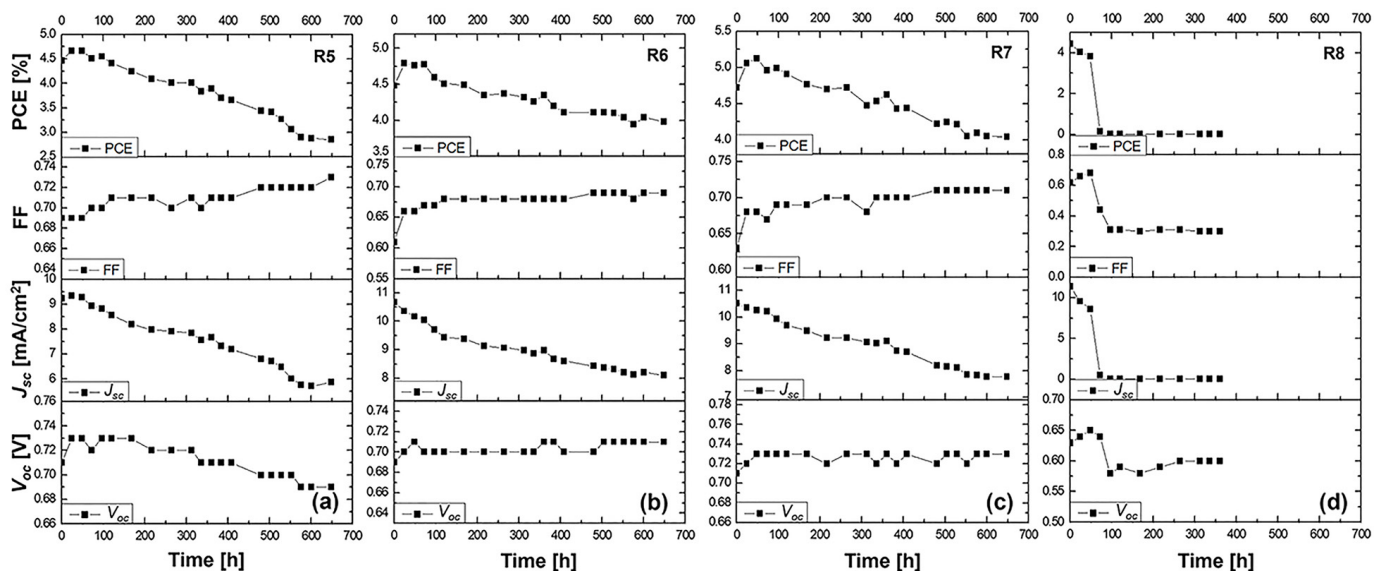


Figure 5. Stability study for more than 600 h at ambient conditions of the (a) R5 DSSC based on the DMPII liquid electrolyte and of the QsDSSCs using PVDF-HFP with different molecular weights: (b) R6—DMPII + PVH70, (c) R7—DMPII + PVH80, and (d) R8—DMPII + PVDH-HFP. All solar cells were sensitized with the N719 dye.

R5 cell (liquid DMPII electrolyte)

The R5 cell, employing a liquid DMPII electrolyte, exhibited a significant 35% efficiency reduction after 600 h. This decline primarily stemmed from the substantial 36% decrease in the J_{sc} , indicating a significant loss in the cell's ability to generate a current from incident light. This could be attributed to several factors, including dye degradation, electrolyte decomposition, or increased charge recombination at the TiO₂/dye/electrolyte interface. The 6% decrease in the V_{oc} suggests increased recombination losses, further supporting this hypothesis. However, the 6% increase in the FF implies improvements in charge transport and collection within the device, possibly due to changes in the electrolyte's conductivity or interfacial properties over time.

R6 cell (PVDF-HFP electrolyte with M.W. of 86,000 g/mol)

Incorporating PVDF-HFP polymers into the electrolyte significantly influenced the devices' stability. The R6 cell, with a polymer molecular weight of 86,000 g/mol, displayed a much smaller efficiency reduction of 11% after 600 h compared to the R5 cell. This improved stability is promising and can be attributed to the polymer's ability to mitigate some degradation pathways present in the liquid electrolyte system. The 3% increase in the V_{oc} suggests a slight reduction in recombination losses, potentially due to the polymer's passivation effect at the TiO₂/dye/electrolyte interface. The 10% increase in the FF indicates improved charge transport and collection, likely facilitated by the polymer's influence on the electrolyte's ionic conductivity and interfacial properties. However, the 25% decrease in the J_{sc} , while less severe than in the R5 cell, still points to some degree of dye degradation or hindered charge injection/regeneration processes.

R7 cell (PVDF-HFP electrolyte with M.W. of 90,000 g/mol)

The R7 cell, employing a slightly higher molecular weight of PVDF-HFP (90,000 g/mol), demonstrated a 15% efficiency reduction after 600 h, slightly higher compared to the R6 cell. This suggests that this specific molecular weight might not offer significant advantages over

the 86,000 g/mol polymer in terms of long-term stability. The 3% increase in the V_{oc} and 13% increase in the FF show similar trends to the R6 cell, indicating potential benefits in reducing recombination and improving charge transport. However, the 25% decrease in the J_{sc} remains a concern, suggesting that the further optimization of the electrolyte composition or device architecture is necessary.

R8 cell (PVDF-HFP electrolyte with M.W. of 455,000 g/mol)

The R8 cell, incorporating the highest molecular weight of PVDF-HFP (455,000 g/mol), suffered a catastrophic failure, with both the efficiency and J_{sc} dropping to zero after 600 h. This dramatic decline clearly demonstrates the detrimental effects of using an excessively high molecular weight of the polymer in the electrolyte. The high molecular weight likely leads to a highly viscous electrolyte, severely hindering ion transport and effectively shutting down charge collection within the device. This is further evidenced by the substantial 54% decrease in the FF, indicating extremely poor charge transport and collection. The 9% decrease in the V_{oc} , despite the complete loss of current generation, suggests that the recombination processes are not the primary cause of the failure in this case.

3.5. DSSCs with Organic Phenothiazine Dye 2-LBH-92 and with and without PVDF-HFP with Different Molecular Weights in DMPII Electrolyte

3.5.1. UV-Vis Absorption and IPCE Spectra

The phenothiazine dye in question, characterized by a long alkoxy side chain and cyanoacrylic acid anchoring group, was designed for efficient light harvesting and electron transfer in DSSCs. The UV-Vis absorption spectrum shown in Figure 6a exhibits a characteristic broad absorption band in the visible region, given the extended π -conjugation and donor-acceptor nature of the molecule, translating into significant photon capture within the spectral range where the solar irradiance is high. This band arises from the intramolecular charge transfer (ICT) between the phenothiazine donor and the cyanoacrylic acid acceptor. The position and intensity of this ICT band are sensitive to the surrounding medium's polarity and can be influenced by the presence of the PVDF-HFP polymer [24]. Additionally, 2-LBH-92 shows a prominent absorption band in the UV region, attributed to π - π^* transitions within the conjugated phenothiazine and phenyl rings.

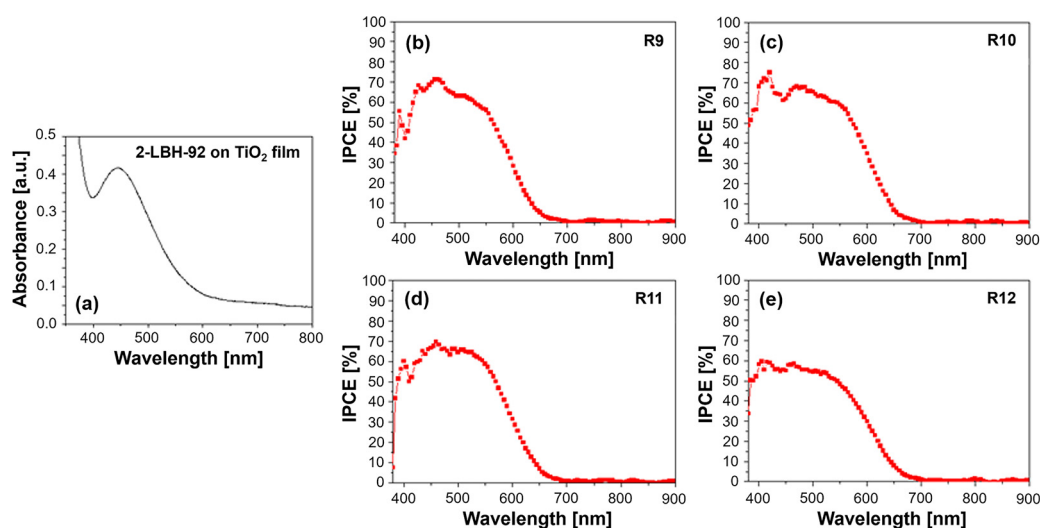


Figure 6. (a) UV-Vis absorption spectrum of 2-LBH-92 organic dye on TiO_2 film and quantum efficiency spectra for (b) R9—DMPII, (c) R10—DMPII + PVH70, (d) R11—DMPII + PVH80, and (e) R12—DMPII + PVDH-HFP 2-LBH-92 sensitized solar cells.

Incorporating PVDF-HFP into the DMPII electrolyte can induce changes in the UV-Vis spectra. For instance, interactions between the dye molecules and the polymer chains might lead to slight shifts in the absorption peaks, reflecting changes in the energy levels within the

dye. Additionally, variations in peak intensity can occur, potentially indicating alterations in the dye’s molar extinction coefficient or aggregation state. Higher-molecular-weight PVDF-HFP might lead to increased viscosity and reduced dye aggregation, potentially enhancing the light absorption. The IPCE spectra provide a direct measure of the DSSCs’ ability to convert absorbed photons into a current. Meanwhile, 2-LBH-92, with its broad absorption profile, is expected to show a correspondingly broad IPCE spectrum, with peaks aligning with its UV and visible absorption bands. The presence of different molecular weights of PVDF-HFP in the electrolyte can significantly influence the IPCE spectra (see Figure 6b–e). Lower-molecular-weight PVDF-HFP, due to its lower viscosity, might facilitate faster ion transport within the electrolyte, leading to more efficient charge collection and potentially higher IPCE values, especially in the longer wavelength regions, where charge recombination becomes more prominent. However, excessively low molecular weights might compromise the quasi-solid-state nature of the electrolyte, negatively impacting its long-term stability.

Conversely, higher-molecular-weight PVDF-HFP, while potentially enhancing the stability, might hinder ion transport due to increased viscosity. This could lead to lower IPCE values, particularly at longer wavelengths, as charge recombination outcompetes charge collection. However, the reduced dye aggregation potentially offered by higher-molecular-weight PVDF-HFP could partially offset this effect by improving the light harvesting. Furthermore, the interaction between the 2-LBH-92 dye and the PVDF-HFP polymer can influence the electron injection and dye regeneration processes. Favorable interactions could facilitate electron injection from the dye’s excited state into the TiO₂ conduction band, leading to increased IPCE values. Conversely, unfavorable interactions could hinder these processes, negatively impacting the device performance.

3.5.2. Stability Study

The stability study of the DSSCs using the phenothiazine organic dye 2-LBH-92 with the liquid DMPII electrolyte and PVDF-HFP polymer electrolytes at different molecular weights is shown in Figure 7.

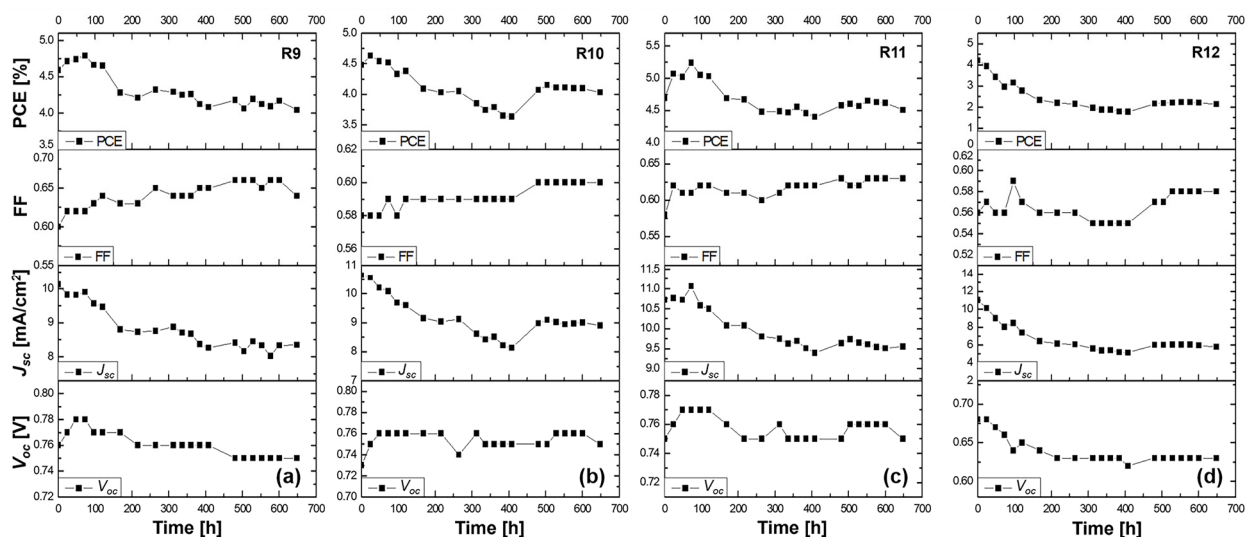


Figure 7. Stability study for more than 600 h at ambient conditions of the (a) R9 DSSC based on the DMPII liquid electrolyte and of the QsDSSCs using PVDF-HFP with different molecular weights: (b) R10—DMPII + PVH70, (c) R11—DMPII + PVH80, and (d) R12—DMPII + PVDH-HFP. All solar cells were sensitized with the phenothiazine organic dye 2-LBH-92.

R9 cell (liquid DMPII electrolyte)

The R9 cell, employing a liquid DMPII electrolyte, exhibited a 12% efficiency reduction after 600 h. This decline primarily stemmed from the 21% decrease in the J_{sc} , indicating

a significant loss in the cell's ability to generate a current from incident light. This could be attributed to several factors, including dye degradation, electrolyte decomposition, or increased charge recombination at the TiO_2 /dye/electrolyte interface. The 3.8% decrease in the V_{oc} further supports this hypothesis, suggesting increased recombination losses. However, the 9% increase in the FF implies improvements in charge transport and collection within the device, possibly due to changes in the electrolyte's conductivity or interfacial properties over time.

R10 cell (PVDF-HFP electrolyte with M.W. of 86,000 g/mol)

Incorporating PVDF-HFP polymers into the electrolyte significantly influenced the devices' stability. The R10 cell, with a polymer molecular weight of 86,000 g/mol, displayed an 11% efficiency reduction after 600 h, comparable to the R9 cell. This suggests that this specific molecular weight might not offer significant advantages in overall efficiency retention compared to the liquid electrolyte. However, a closer look at the individual parameters reveals a more nuanced picture. The 4% increase in the V_{oc} suggests a reduction in recombination losses, potentially due to the polymer's passivation effect at the TiO_2 /dye/electrolyte interface. The substantial 33% increase in the FF indicates significantly improved charge transport and collection, likely facilitated by the polymer's influence on the electrolyte's ionic conductivity and interfacial properties. This improvement in the FF partially compensates for the 16% decrease in the J_{sc} , which, while still present, is less severe than in the R9 cell. This suggests that the polymer might be mitigating some degradation pathways affecting J_{sc} , even if not completely eliminating them.

R11 cell (PVDF-HFP electrolyte with M.W. of 90,000 g/mol)

The R11 cell, employing a slightly higher molecular weight of PVDF-HFP (90,000 g/mol), demonstrated the most promising stability results, with only a 4% efficiency reduction after 600 h. This suggests that this specific molecular weight might offer a trade-off in balancing the benefits of polymer incorporation with minimal adverse effects on performance. The 5% decrease in the V_{oc} , while indicating some increase in recombination, is less pronounced than in the R9 cell. The 8% increase in the FF, while not as dramatic as in the R10 cell, still points to improved charge transport and collection. The 15% decrease in the J_{sc} , comparable to the R10 cell, suggests that the polymer's influence in terms of mitigating the J_{sc} degradation pathways might be similar for both molecular weights.

R12 cell (PVDF-HFP electrolyte with M.W. of 455,000 g/mol)

The R12 cell, incorporating the highest molecular weight of PVDF-HFP (455,000 g/mol), suffered a significant 50% efficiency reduction after 600 h, the most severe among all tested cells. This clearly demonstrates the detrimental effects of using a polymer with an excessively high molecular weight in the electrolyte. The high molecular weight likely leads to a highly viscous electrolyte, severely hindering ion transport and negatively impacting charge collection within the device. This is further evidenced by the relatively small 3.5% increase in the FF, indicating a limited improvement in charge transport compared to the lower-molecular-weight polymers. The 8% decrease in the V_{oc} and the substantial 46% decrease in the J_{sc} further highlight the negative impact of the high-molecular-weight polymer on both the recombination losses and charge generation/collection processes.

In summary, the alterations of the V_{oc} , J_{sc} , FF, and overall efficiency in these cells over time provided insights into how the molecular weight of the PVDF-HFP polymer electrolytes could severely influence the long-term performance of DSSCs. The changes observed in the solar cell parameters suggested a trade-off between the structural and transport properties of the polymers used. Lower molecular weights seemed to favor a more stable interface and better transport properties, leading to a smaller decrease in efficiency, whereas very high-molecular-weight polymers may impede ion movement and increase recombination, significantly reducing the cell's performance.

4. Discussion

This study aimed to provide a comprehensive analysis of the impact of incorporating poly(vinylidene fluoride-co-hexafluoropropylene) with varying molecular weights into

the liquid DMPII electrolyte of DSSCs. Three different dyes, namely the commercially available ruthenium-based Z907 and N719 and the organic phenothiazine dye 2-LBH-92, were investigated to understand how the polymer–electrolyte interaction influences device performance and stability across different dye systems.

Our findings highlight the complex interplay between the dye structure, polymer molecular weight, and resulting electrolyte properties on the overall device performance. While all DSSCs exhibited a decrease in efficiency after 600 h, the extent of the degradation and the underlying mechanisms differed significantly depending on the specific dye and polymer combination. Cells employing the liquid DMPII electrolyte, regardless of the dye, generally exhibited more pronounced efficiency reductions compared to their counterparts incorporating PVDF-HFP. This observation underscores the inherent limitations of liquid electrolytes in terms of long-term stability, likely due to factors like dye desorption, electrolyte decomposition, and increased interfacial recombination.

Incorporating PVDF-HFP into the electrolyte yielded varying results depending on the dye and polymer molecular weight. For the Z907 and N719 dyes, incorporating PVDF-HFP generally led to improved stability compared to the liquid electrolyte, particularly at specific molecular weights. This improvement can be attributed to several factors, including (1) enhanced interfacial stability—the polymer could passivate the TiO_2 /dye/electrolyte interface, reducing recombination losses and improving the V_{oc} , as observed in several cases; (2) improved ionic conductivity—the polymer might influence the electrolyte's ionic conductivity, facilitating charge transport and enhancing the FF, as evidenced by the observed increases in this parameter.

For all dye–polymer combinations, the polymer might have hindered dye aggregation on the TiO_2 surface, leading to better dye regeneration and improved J_{sc} retention. However, the optimal molecular weight for PVDF-HFP varied depending on the dye. This suggests that the polymer's interaction with the dye molecules and its influence on the overall electrolyte environment are crucial factors in determining the device's stability. The 2-LBH-92 dye, when paired with PVDF-HFP, exhibited more complex behavior. While some molecular weights led to improved stability compared to the liquid electrolyte, others resulted in more severe degradation. This suggests a more intricate interplay between the 2-LBH-92 dye structure and the polymer, potentially involving specific interactions that influence dye aggregation, electron injection, or the recombination dynamics. The most significant observation across all dyes was the detrimental effect of using an excessively high molecular weight of PVDF-HFP. This consistently led to a substantial decrease in efficiency, primarily driven by a significant drop in the J_{sc} and FF. This result highlights the importance of balancing the beneficial properties of the polymer, such as enhanced interfacial stability, with its potential drawbacks, such as increased viscosity and hindered ion transport, which become particularly problematic at high molecular weights.

The decrease in J_{sc} over time can be attributed to several dye degradation mechanisms. For the dyes investigated (Z907, N719, and the phenothiazine dye), prolonged illumination and specific electrolyte environments can lead to degradation pathways such as photo-oxidation, dye desorption, and chemical interactions with the electrolyte components. Photo-oxidation occurs when dyes are exposed to light over extended periods, leading to their breakdown and a reduced ability to absorb photons. Dye desorption involves the detachment of the dye molecules from the TiO_2 surface, diminishing the number of active sites for electron injection. Additionally, chemical interactions between the dye and electrolyte components can result in the formation of inactive complexes, further decreasing the J_{sc} . The influence of PVDF-HFP gel polymer electrolytes with different molecular weights on J_{sc} decay has also been explored. The polymer structure and properties, such as ion mobility and long-term stability, play crucial roles in this context. High-molecular-weight polymers can impede ion movement, affecting the efficiency of charge transport within the cell. Conversely, lower-molecular-weight polymers might enhance ion mobility but could compromise the overall stability of the electrolyte, leading to degradation over time. Charge transport limitations within the device are another critical factor impacting the

J_{sc} . Changes in charge transport properties, including electrolyte degradation, interface modifications, and increased recombination processes, can hinder electron injection and transport. Electrolyte degradation reduces the ionic conductivity, while interfacial modifications between the dye and TiO_2 can create traps for electrons, leading to increased recombination. These factors collectively contribute to a gradual decline in J_{sc} , highlighting the importance of optimizing both the dye stability and electrolyte properties to enhance the long-term performance of DSSCs.

In conclusion, our study demonstrates the critical role of carefully selecting the appropriate polymer molecular weight and considering its interaction with the specific dye employed in QsDSSCs. While incorporating PVDF-HFP can enhance the stability compared to liquid electrolytes, optimizing the polymer molecular weight for the chosen dye is crucial to maximize the device performance and longevity. This study provides valuable insights for the development of efficient and stable QsDSSCs for future applications.

5. Conclusions

The performance of QsDSSCs is critically dependent on the intricate interplay between the photosensitizing dye, the semiconductor, and the quasi-solid electrolyte. The choice of dye, particularly its energy level alignment with the TiO_2 semiconductor, significantly influences the charge injection, the recombination dynamics, and, ultimately, the overall efficiency of the device. Dyes like N719 and Z907, with their established performance in DSSCs, provide a good baseline for comparison. However, organic dyes, such as the phenothiazine dye investigated in this study, offer potential advantages in terms of tunable optoelectronic properties and cost-effectiveness. The careful molecular engineering of these dyes is essential to optimize their energy levels for efficient electron injection and reduced recombination in the context of a quasi-solid-state electrolyte. The quasi-solid electrolyte, while offering advantages in terms of stability and leakage prevention, introduces additional complexities. The slower diffusion of ions within the more viscous medium necessitates a highly efficient charge transfer process at the dye–semiconductor interface. Phenothiazine dye-based QsDSSCs showed promising stability for longer durations of time compared with the Z907 and N719 dyes. Future research should focus on tailoring both the dye structure and the electrolyte composition to create synergistic interactions that maximize charge transport and minimize recombination losses, paving the way for high-performance, stable, and commercially viable QsDSSCs.

Author Contributions: Conceptualization, R.A.A., K.Y.R., W.S.S. and D.P.; methodology, R.A.A., K.Y.R., W.S.S. and D.P.; formal analysis, R.A.A., K.Y.R., W.S.S. and D.P.; data curation, R.A.A., K.Y.R. and W.S.S.; writing—original draft preparation, R.A.A., W.S.S. and D.P.; writing—review and editing, R.A.A., W.S.S. and D.P.; visualization, R.A.A., W.S.S. and D.P.; supervision, W.S.S.; project administration, R.A.A. and W.S.S.; funding acquisition, R.A.A. and W.S.S. All authors have read and agreed to the published version of the manuscript.

Funding: This study was supported by the Converging Research Center Program through the Ministry of Education, Science and Technology (2010K000970), Republic of Korea.

Data Availability Statement: Data available on request due to privacy restrictions.

Acknowledgments: R.A.A. would like to thank Sunandan Baruah for the fruitful discussions. D.P. acknowledges the support from the European Union—NextGenerationEU, under the National Recovery and Resilience Plan (NRRP), Mission 04 Component 2 Investment 3.1, Project Code: IR0000027—CUP: B33C22000710006—iENTRANCE@ENL: Infrastructure for Energy Transition and Circular Economy @ EuroNanoLab.

Conflicts of Interest: The authors declare no conflicts of interest.

References

1. O'Regan, B.; Grätzel, M. A low-cost, high-efficiency solar cell based on dye-sensitized colloidal TiO₂ films. *Nature* **1991**, *353*, 737–740. [[CrossRef](#)]
2. Wang, P.; Zakeeruddin, S.M.; Moser, J.E.; Nazeeruddin, M.K.; Sekiguchi, T.; Grätzel, M. A stable quasi-solid-state dye-sensitized solar cell with an amphiphilic ruthenium sensitizer and polymer gel electrolyte. *Nat. Mater.* **2003**, *2*, 402–407. [[CrossRef](#)]
3. Kim, M.-R.; Jin, S.-H.; Park, S.-H.; Lee, H.-J.; Kang, E.-H.; Lee, J.-K. Photovoltaic properties and preparations of dye-sensitized solar cells using solid-state polymer electrolytes. *Mol. Cryst. Liq. Cryst.* **2006**, *444*, 233–239. [[CrossRef](#)]
4. Lan, Z.; Wu, J.; Wang, D.; Hao, S.; Lin, J.; Huang, Y. Quasi-solid state dye-sensitized solar cells based on gel polymer electrolyte with poly(acrylonitrile-co-styrene)/NaI+I₂. *Sol. Energy* **2006**, *80*, 1483–1488. [[CrossRef](#)]
5. Chung, I.; Lee, B.; He, J.; Chang, R.P.H.; Kanatzidis, M.G. All-solid-state dye-sensitized solar cells with high efficiency. *Nature* **2012**, *485*, 486–489. [[CrossRef](#)] [[PubMed](#)]
6. Li, S.; Qiu, L.; Shi, C.; Chen, X.; Yan, F. Water-resistant, solid-state, dye-sensitized solar cells based on hydrophobic organic ionic plastic crystal electrolytes. *Adv. Mater.* **2014**, *26*, 1266–1271. [[CrossRef](#)] [[PubMed](#)]
7. Bai, Y.; Cao, Y.; Zhang, J.; Wang, M.; Li, R.; Wang, P.; Zakeeruddin, S.M.; Grätzel, M. High-performance dye-sensitized solar cells based on solvent-free electrolytes produced from eutectic melts. *Nat. Mater.* **2008**, *7*, 626–630. [[CrossRef](#)] [[PubMed](#)]
8. Lu, W.; Fadeev, A.G.; Qi, B.; Smela, E.; Mattes, B.R.; Ding, J.; Spinks, G.M.; Mazurkiewicz, J.; Zhou, D.; Wallace, G.G.; et al. Use of ionic liquids for π -conjugated polymer electrochemical devices. *Science* **2002**, *297*, 983–987. [[CrossRef](#)]
9. Shibli, H.M.; Hafez, H.S.; Rifai, R.I.; Abdel Mottaleb, M.S.A. Environmental friendly, low cost quasi solid state dye sensitized solar cell: Polymer electrolyte introduction. *J. Inorg. Organomet. Polym. Mater.* **2013**, *23*, 944–949. [[CrossRef](#)]
10. ElBatal, H.S.; Aghazada, S.; Al-Muhtaseb, S.A.; Grätzel, M.; Nazeeruddin, M.K. Quasi-solid-state dye-sensitized solar cells based on Ru(II) polypyridine sensitizers. *Energy Technol.* **2016**, *4*, 380–384. [[CrossRef](#)]
11. Gong, J.; Sumathy, K.; Liang, J. Polymer electrolyte based on polyethylene glycol for quasi-solid state dye sensitized solar cells. *Renew. Energy* **2012**, *39*, 419–423. [[CrossRef](#)]
12. Cleghorn, S.J.C.; Mayfield, D.K.; Moore, D.A.; Moore, J.C.; Rusch, G.; Sherman, T.W.; Sisofo, N.T.; Beuscher, U. A polymer electrolyte fuel cell life test: 3 years of continuous operation. *J. Power Sources* **2006**, *158*, 446–454. [[CrossRef](#)]
13. Collier, A.; Wang, H.; Yuan, X.Z.; Zhang, J.; Wilkinson, D.P. Degradation of polymer electrolyte membranes. *Int. J. Hydrogen Energy* **2006**, *31*, 1838–1854. [[CrossRef](#)]
14. Arof, A.K.; Naeem, M.; Hameed, F.; Jayasundara, W.J.M.J.S.R.; Careem, M.A.; Teo, L.P.; Buraidah, M.H. Quasi solid state dye-sensitized solar cells based on polyvinyl alcohol (PVA) electrolytes containing I⁻/I₃⁻ redox couple. *Opt. Quantum Electron.* **2014**, *46*, 143–154. [[CrossRef](#)]
15. Venkatesan, S.; Liu, I.-P.; Tseng Shan, C.-M.; Teng, H.; Lee, Y.-L. Highly efficient indoor light quasi-solid-state dye sensitized solar cells using cobalt polyethylene oxide-based printable electrolytes. *Chem. Eng. J.* **2020**, *394*, 124954. [[CrossRef](#)]
16. Sultana, M.; Mehmood, U.; Nazar, R.; Gill, Y.Q. Development of multiwalled carbon nanotubes/polyaniline nanocomposites based electrolyte for quasi-solid-state dye-sensitized solar cells. *Int. J. Energy Res.* **2022**, *46*, 9911–9918. [[CrossRef](#)]
17. Aftab, S.; Iqbal, M.Z.; Hussain, S.; Kabir, F.; Hegazy, H.H.; Goud, B.S.; Aslam, M.; Xu, F. MXene-modified electrodes and electrolytes in dye-sensitized solar cells. *Nanoscale* **2023**, *15*, 17249–17269. [[CrossRef](#)] [[PubMed](#)]
18. Venkatesan, S.; Lin, W.-H.; Teng, H.; Lee, Y.-L. High-efficiency bifacial dye-sensitized solar cells for application under indoor light conditions. *ACS Appl. Mater. Interfaces* **2019**, *11*, 42780–42789. [[CrossRef](#)] [[PubMed](#)]
19. Ito, S.; Takahashi, K.; Yusa, S.-I.; Saito, M.; Shigetomi, T. Ultradurable dye-sensitized solar cells under 120 °C using cross-linkage dye and ionic-liquid electrolyte. *Int. J. Photoenergy* **2013**, *2013*, 501868. [[CrossRef](#)]
20. Nguyen, P.T.; Lam, B.X.T.; Andersen, A.R.; Hansen, P.E.; Lund, T. Photovoltaic performance and characteristics of dye-sensitized solar cells prepared with the N719 thermal degradation products [Ru(LH)₂(NCS)(4-*tert*-butylpyridine)][N(Bu)₄] and [Ru(LH)₂(NCS)(1-methylbenzimidazole)][N(Bu)₄]. *Eur. J. Inorg. Chem.* **2011**, *2011*, 2533–2539. [[CrossRef](#)]
21. Al-Mohsin, H.A.; Mineart, K.P.; Armstrong, D.P.; El-Shafei, A.; Spontak, R.J. Quasi-solid-state dye-sensitized solar cells containing a charged thermoplastic elastomeric gel electrolyte and hydrophilic/phobic photosensitizers. *Sol. RRL* **2018**, *2*, 1700145. [[CrossRef](#)]
22. Venkatesan, S.; Liu, I.-P.; Li, C.-W.; Tseng-Shan, C.-M.; Lee, Y.-L. Quasi-solid-state dye-sensitized solar cells for efficient and stable power generation under room light conditions. *ACS Sustain. Chem. Eng.* **2019**, *7*, 7403–7411. [[CrossRef](#)]
23. Saaïd, F.I.; Tseng, T.-Y.; Winie, T. PVdF-HFP quasi-solid-state electrolyte for application in dye-sensitized solar cells. *Int. J. Technol.* **2018**, *9*, 1187–1195. [[CrossRef](#)]
24. Hua, Y.; Chang, S.; He, J.; Zhang, C.; Zhao, J.; Chen, T.; Wong, W.-Y.; Wong, W.-K.; Zhu, X. Molecular engineering of simple phenothiazine-based dyes to modulate dye aggregation, charge recombination, and dye regeneration in highly efficient dye-sensitized solar cells. *Chem.-A Eur. J.* **2014**, *20*, 6300–6308. [[CrossRef](#)]

Disclaimer/Publisher's Note: The statements, opinions and data contained in all publications are solely those of the individual author(s) and contributor(s) and not of MDPI and/or the editor(s). MDPI and/or the editor(s) disclaim responsibility for any injury to people or property resulting from any ideas, methods, instructions or products referred to in the content.